

Topology Optimization in the Inertial Platform System

Zhang Kai*, Liu Yun, Wang Ting
Beijing Institute of Aerospace Control Device, Beijing, China

Abstract: The supporting bracket for the inertial platform is the key component in launch vehicles. The bracket is supporting the inertial platform during the flight condition of launch vehicles. Thus the axial load is more important than the radial load, which still needs to be considered. Lightweight design is of great significance for such a supporting bracket. In this study, the weight of the initial design of the supporting bracket is 13.8kg, however, the allowed weight is only limited to 8.0kg. Since the material is restricted to be the aluminum alloy, the problem is to seek the optimized topology design with a weight constraint of 8.0kg. Obtaining the loading path and removing the inefficient material in the supporting bracket can be solved by the topology optimization. The weighted multi-load cases topology optimization is utilized due to the different load conditions. The rectangle space and the circle space which are two different kinds of initial design space are given and the topology optimized results are similar in the software of OptiStruct, where the topology optimization algorithm is the SIMP (Solid Isotropic Material with Penalization) method. Considering these two topology optimum results, the new model of the supporting bracket is designed. The simulation analysis comparisons of the two models (before and after optimization) including the static, modal analysis (including constrained and free), frequency response analysis and random analysis are carried out. The weight of the final optimum model is reduced to about 8.0kg for the new design. Even through the maximum Von Mises stress in the optimum model in one load case is larger than that of the initial model, but the value of the maximum is much smaller than the yield strength of the material aluminum alloy. But for the other load cases, the maximum Von Mises stress is much lower than that of the initial model, and the stress distribution of the supporting bracket is more uniformly due to the improved material utilization by the structural optimization.

Keywords: Inertial Platform System; Supporting Bracket; Topology Optimization; Simulation Analysis

1. Introduction

The inertial platform provides the positions and attitudes of launch vehicles in the flight which is the key component of the inertial navigation. The supporting bracket supporting inertial platform in the launch vehicles provides the great environment for the inertial platform which means the enough stiffness, enough strengthen and enough stability.

In the aerospace field, the weight is much valuable. Less weight means more benefit. On the contrary, more weight as well as the more material brings the higher mechanical performance for the product. It seems a contradiction for obtaining the less material and the higher mechanical performance.

In this paper, the allowed weight of the supporting bracket is limited to 8.0kg, while the initial weight of the supporting bracket is 13.8kg. The material is restricted to be the aluminum alloy. We have to reduce the weight on the condition with the stratification of the mechanical performance of the supporting bracket. The basic idea is to increase the utility of the material, remove the useless material. Thus the problem is to seek the optimized topology design with a weight constraint of 8.0kg. Obtaining the loading path and removing the inefficient material in the supporting bracket can be solved by the topology optimization.

In applications regarding component design of aerospace and aeronautical structures, topology optimization has been employed for improving the structural and multi-disciplinary behaviors, such as overall stiffness, aerodynamic performance and fundamental frequencies under specified structural weight constraint. Krog and Tuck [1] applied the topology optimization techniques to the optimal design of aircraft wing-box ribs. Chen et al. [2] obtained the minimized weight on the constraint of the modal frequencies in structural design of the spacecraft based on NASTRAN. Maute and Allen [3] presented a material density-based approach for the optimal placement of stiffeners in a flexible wing subject to aerodynamic forces. The material distribution formulation has also been used by Maute and Reich [4] in the optimal design of actuator locations and the inner structures of adaptive wings. Afonso et al. [5] combined the topology optimization and the shape optimization for the design of stiffened shell structures, which have been widely used in the aerospace industry. Yin et al. [6] reduced the heat shield weight by 8.0% with the sequential quadratic programming (SQP) algorithm on the consideration of the first order frequency as the constraint. Kang et al. [7] achieved the topology optimization results of the space vehicle structures considering attitude control effort. Chen et al. [8] applied topology optimization techniques in the layout design of stiffeners in a storage tank of a

space craft for minimum weight under stiffness and strength constraints.

In this paper, the weighted multi-load cases topology optimization is applied due to the different load conditions. The weight of the final optimum model is reduced to about 8.0kg. The simulation analysis comparisons of the two models (before and after optimization) including the static analysis, modal analysis (including constrained and free conditions), frequency response analysis and random analysis are carried out. Even through the maximum Von Mises stress in the optimum model in one load case is larger than that of the initial model, but the value of the maximum is much smaller than the yield strength of the material aluminum alloy. But for the other load cases, the maximum Von Mises stress is much lower than that of the initial model, and the stress distribution of the supporting bracket is more uniformly due to the improved material utilization by the structural optimization.

2. Structural Optimization

2.1 Numerical model

The 3D geometry model of the supporting bracket is imported from ProE and the finite element model (FEM) is built in Hypermesh. The supporting bracket is fastened by the bolts which are simulated by the RBE2 element in OptiStruct in which the displacements of the slave nodes are consistent with that of the master node. The RBE3 element is chosen to connect the node which located in the centroid of the inertial platform and the master nodes from the RBE2 elements in the supporting bracket. The Tetra10 is taken to mesh the model where the nodes are 187842 and the elements are 105391 including 1 RBE3 element and 16 RBE2 element.

The material of the supporting bracket is aluminum alloy whose properties are shown in Table 1. The mass of the supporting bracket is 13.8Kg.

Table 1. Material properties of aluminum alloy

Young's modulus (MPa)	7E4
Poisson's ratio	0.33
Density(t/mm ³)	2.67E-9

The displacement constraints are fixed 6 degrees of the freedom of the mater nodes of the RBE2 elements in the underside of the supporting bracket, as shown in Fig.1. Three force loads are applied in the centroid node of the inertial platform which the amplitude is 1E4 N in order to simulate the overload load case. The direction of the force loads are along the negative direction of the three axes. The x-axis is the axial direction of the supporting bracket and the y-axis and z-axis are the radial directions of the supporting bracket.

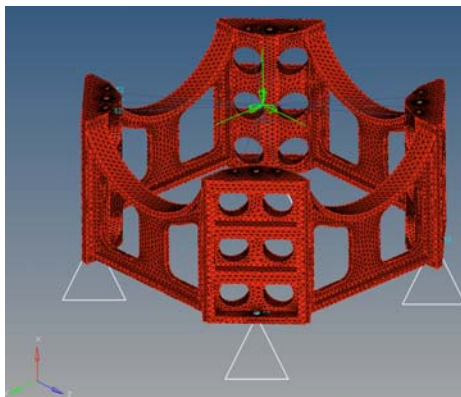


Fig.1. The FEM of the initial model

2.2 Topology optimization

In order to achieve the highest global stiffness of the structure in each load case with the lower material, the weighted multi-load cases topology optimization is carried out. Conventionally, topology optimization of continuum structures in the multi-load cases is formulated as a minimum mean compliance problem under a material volume

constraint. In the SIMP formulation, an artificial isotropic material model is introduced and element-wise material density variables are used for describing the structural layout. To suppress the intermediate densities in the resulting optimum design, a penalized interpolation scheme between Young's modulus E and the material density x is assumed as

$$E = x^p E_0 \quad (1)$$

where p is the penalty factor, where $p > 1$, E_0 is the Young's modulus of the fully solid material, which has a unit density.

In this study, the topology optimization problem with a volume constraint is expressed as

$$\begin{aligned} C(\mathbf{X}) &= \sum_i^g \frac{1}{g} c_i(\mathbf{X}) \\ \min_x \quad &= \sum_i^g \frac{1}{g} \mathbf{U}_i^T \mathbf{K}_i \mathbf{U}_i \\ &= \sum_i^g \sum_{e=1}^N \frac{1}{g} ((x_e)^p \mathbf{u}_e^T \mathbf{k}_e^0 \mathbf{u}_e)_i \end{aligned} \quad (2)$$

$$\text{subject to } \frac{V(x)}{V_0} = f_v$$

$$0 < x_{\min} \leq x_e \leq x_{\max} = 1, e = 1, 2, \dots, N$$

where c represents the strain energy, g means the number of load cases, x_e denotes the density of the e -th element, \mathbf{X} is the vector of elemental design variables, \mathbf{K} is the global stiffness matrix, \mathbf{U} is the vector of nodal displacement, \mathbf{u}_e denotes the elemental displacement vector, \mathbf{k}_e^0 is the stiffness matrix of the e -th element when it is made of the solid material, N is the total number of elements, V is the material volume, V_0 is the design domain volume, f_v is the prescribed volume fraction. In order to avoid the numerical difficulties caused by non-positive definite stiffness matrix, a lower-bound limit $x_{\min} > 0$ is imposed on the material density.

The rectangle space and the circle space which are two different kinds of initial design space are given, as shown in Fig.2. The design variables are all the solid elements. The optimization constraint is the volume fraction limited to 15%. The optimization objective is minimizing the weighted global compliance in which the coefficient of the axial load case is 0.6, while those of other load cases are 0.2.

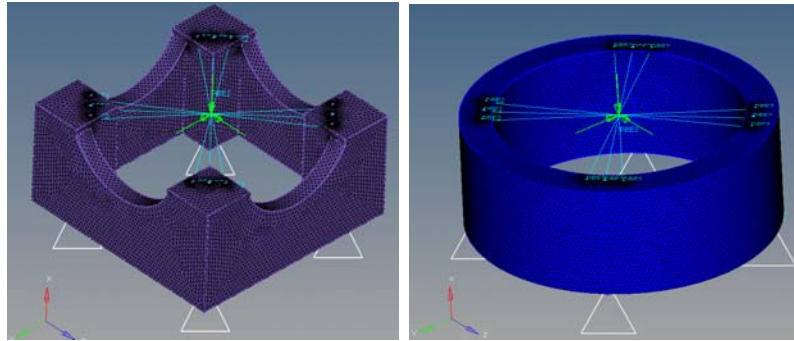


Fig.2. The rectangle space (left) and the circle space

The displacement and force load boundary conditions are the same as Section 2.1. Considering the manufacture constraint, the minimum element is 20mm and two symmetrical plane are given. The symmetrical planes whose normal are y-axis and z-axis individually are both getting through the centroid node of the inertial platform.

In each kind of the initial design space, model 1 is taking RBE2 element to couple centroid node of the inertial platform. Model 2 is taking RBE3 element to couple centroid node of the inertial platform. Model 3 based on model 1 is introduced the constraint of x-axis drawing. The topology optimization is calculated in OptiStruct.

The topology results are shown in Fig.3 and Fig.4, respectively. First of all, the results of model 3 are not available due to many void elements. The results of model 1 and model 2 are much similar. So the characteristics from the model 1 and model 2 are taken into consideration.

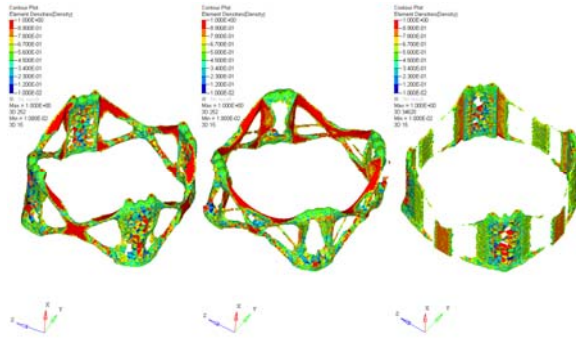


Fig.3. The topology optimum results from the rectangle space

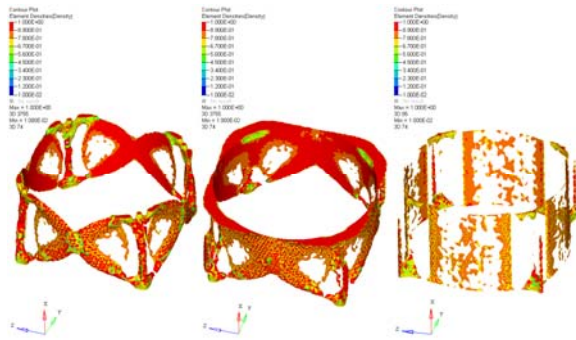


Fig.4. The topology optimum results from the circle space

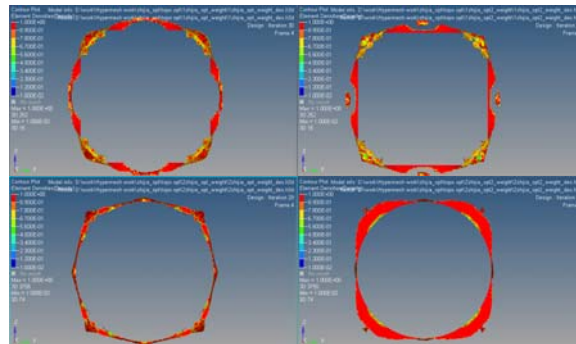


Fig.5. The top view of the topology optimum results from rectangle space (upper figure) and the circle space (lower figure)

As shown in Fig.3 and Fig.4, there seems a crossing pole in one fourth of the model where the shape of the two large void element areas like triangle. The supporting column also exist many void elements in Fig.3 and Fig.4. As can be seen from Fig.5, the top view shape of the topology optimum results is approximating the octahedron.

Based on the characteristics observed, the new design is given as shown in Fig.6. The mass of the new design is 8.1Kg which is by 41.3% lighter than 13.8Kg of the initial design.

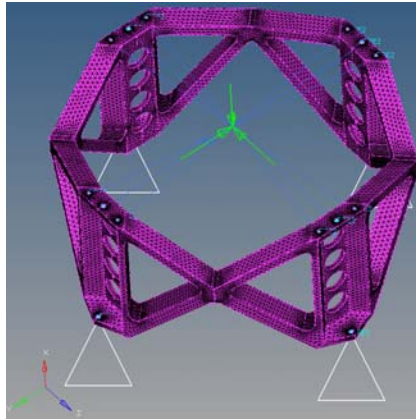


Fig.6. The new design FEM of the supporting bracket

3. Comparisons in Simulation Analysis

3.1 Static analysis

The static analysis is to simulate the overload environment. The mesh grid of all simulation models is the second order which is the Tetra 10 in order to get the relative high precision. The boundary condition is the same as chapter 2. All the simulation analysis is solved in the RADIOSS, the post-processing data is extracted in HyperView.

The element results of the Von Mises are calculated. The elements of the stress singularity whose value is much larger than that of other elements are removed. The element stress contour is shown in Fig.7-Fig.9. The maximum stress and displacement results are given in Table 2.

From the results, the results of the displacement are all very small. The maximum Von Mises stress of the new design is larger than that of the initial design in axial load case. But the value of the new design is much smaller than the yield strength, even much smaller than that of initial design in radial load cases. The placement of the maximum stress is around the bolts which mean the stress concentration causes the high stress. In radial load cases, the distribution of the stress and value of the stress in the new design are both better than those in the initial design.

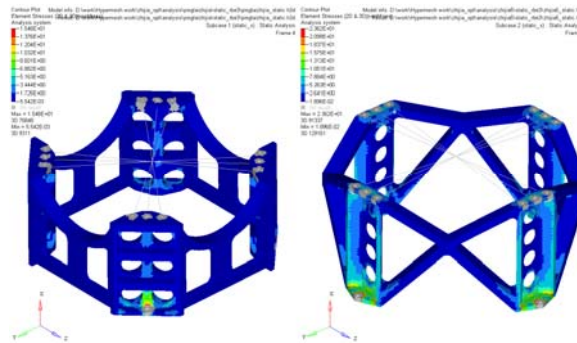


Fig.7. The element Von Mises results of the initial design (left) and new design in axial load case (x-axis)

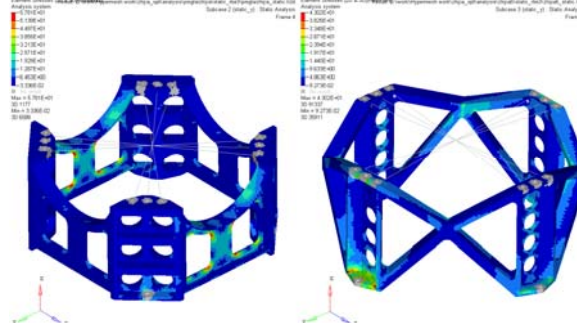


Fig.8. The element Von Mises results of the initial design (left) and new design in radial load case (y-axis)

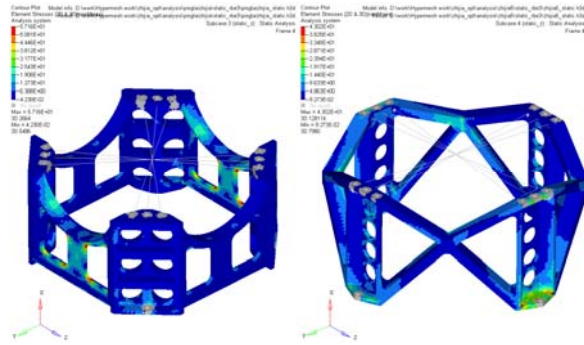


Fig.9. The element Von Mises results of the initial design (left) and new design in radial load case (z-axis)

Table 2. The static analysis results of the initial design and the new design

Model	Max. Von Mises (MPa)	Max. Displacement (mm)
Initial in x-axis	15.48	1.704e-2
New in x-axis	23.62	8.585e-2
Initial in y-axis	57.81	2.466e-1
New in y-axis	43.02	2.773e-1
Initial in z-axis	57.16	2.445e-1
New in z-axis	43.02	2.773e-1

3.2 Modal analysis

The modal analysis is necessary for the structure vibration. The free modal analysis and constraint modal analysis are applied to these two models.

As for the free modal analysis, the seventh order frequency is compared in these two models due to the first sixth rigid body modes. The seventh vibration mode is shown in Fig.10 and the frequency results are given in Table 3. The seventh order frequency of the new design is much larger than that of the initial design which is increasing about 110.8%

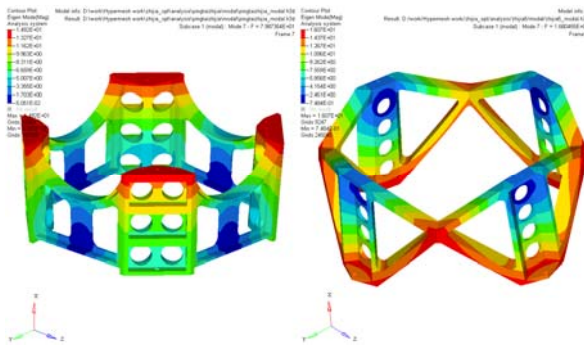


Fig.10. The seventh vibration mode of the initial design (left) and the new design in the free modal analysis

Table 3. The frequency of these two models in free modal analysis

Order	FREQ(Hz) initial	FREQ(Hz) new
7	79.9	168.0
8	180.8	196.3

9	187.1	243.7
---	-------	-------

The constraint modal analysis shows the initial design increase the first frequency after the RBE2 elements are fixed 6 degrees of freedom which 318.3Hz of the initial design is larger than 275.2Hz of the new design. But as shown in Fig.11, the weak region for the initial design which is shown in red color is reinforced in the new design which is show in yellow color.

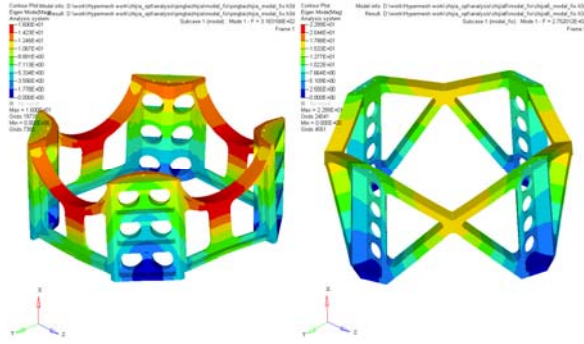


Fig.11. The first vibration mode of the initial design (left) and the new design in the constraint modal analysis

Table 4. The frequency of these two models in constraint modal analysis

Order	FREQ(Hz) initial	FREQ(Hz) new
1	318.3158	275.2012
2	400.7410	512.9752
3	469.0963	533.8597

3.3 Frequency response analysis

The frequency response analysis is simulating the structure dynamic response in the sine sweep excitation. The input sine sweep excitation which is show in Fig.12 is applied in the fixed nodes.

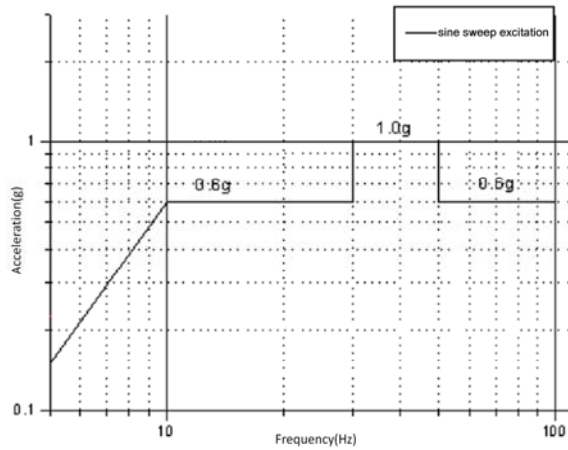


Fig.12. The input sine sweep excitation curve

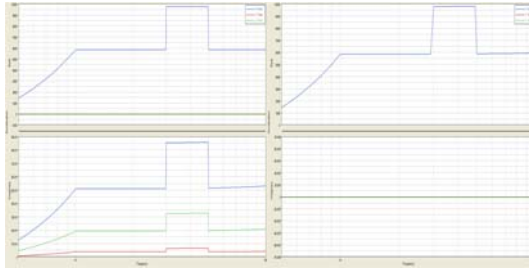


Fig.13. The acceleration curves of the output response node in axial load case (x-axis) in the initial design (left) and in the new design

Fig.13 shows the acceleration curves of output response node in these two models in axial load case which are much similar to the input excitation. These two models have great stiffness to transfer the sine sweep excitation.

3.4 Random analysis

The random analysis is taken to simulate the structure random response in the random excitation such as the environment of the launch vehicle motor working. The input power spectral density (PSD, g^2/Hz) which is imposed in the fixed nodes of these models is given in Fig.14 .

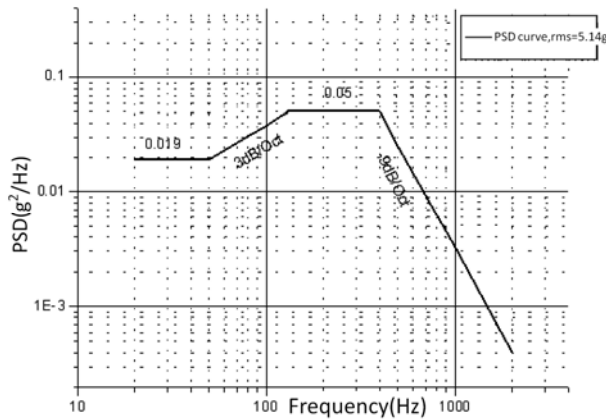


Fig.14. The input PSD curve

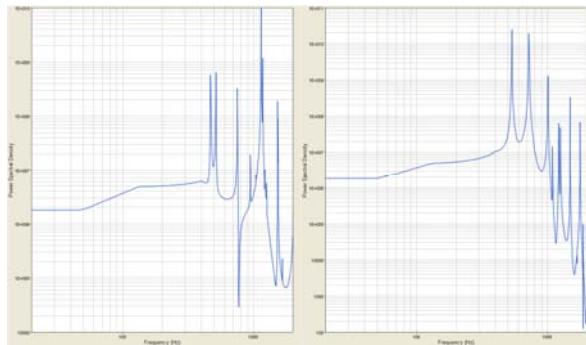


Fig.15. The PSD curves of the output response node in axial load case (x-axis) in the initial design (left) and in the new design

Fig.15 shows the results PSD curves of the output response node in axial load case in these two models. The peak value of the PSD curve in the initial design is obtained in 468.0Hz while that in the new design is obtained in 535.0Hz. The root mean square (RMS) value is given in Table 5 which means the difference is great in the initial design in different load cases, but much more even in the new design. The new design has the similar performance in all the load case but the initial only has great performance in axial load case and much bad in radial load case.

Table 5. The rms value of output nodes in these two models in the random analysis

Output node	RMS(g) x-axis	RMS(g) y-axis	RMS(g) z-axis
In initial design	34.96	119.69	114.24
In new design	60.82	66.87	51.64

4. Conclusions

The supporting bracket for the inertial platform is optimized in order to reduce the weight on the condition of the stratification of the mechanical performance of the supporting bracket. Two different kinds of initial design space is carried out to search for the topology optimum results. The new design which is by 41.3% lighter than 13.8Kg of the initial design is given by the topology optimum results. Simulation analysis is taken to calculate the mechanical performance. In the overload static analysis, the Von Mises stress is more uniformly due to the improved material utilization, while as for the initial design, the maximum stress is small in axial load case, but that is large in radial load case. The same problem occurs in random analysis, the RMS value is small in axial load case, but that is large in radial load case for the initial design, while the RMS value is much even in all the load case for the new design. The free modal analysis show the nature frequency of the new design is much larger that of the initial design. But the constraint modal analysis indicates that the nature frequency of the new design is lower than that of the initial design which the stiffness is much increased due to the imposed fixed constraint. The frequency response analysis means these two models have great stiffness to transfer the sine sweep excitation. In the future, the shape or sizing optimization needs to improve the frequency of the constraint modal analysis. Other optimization methods can be used to optimize the vibration performance in the random vibration condition.

5. References

- [1] Krog L.A. and Tuck K., Topology optimization of aircraft wing box ribs, AIAA, (2004)2004-4481.
- [2] Chen S. Y., Wang W. and Li J. H. Y., Development of topology optimization system based on Msc.Patran/Nastran, CJK-OSM7. Huangshan, China, June 2012.
- [3] Maute K. and Allen M., Conceptual design of aeroelastic structures by topology optimization, Structural and Multidisciplinary Optimization, 27(1-2) (2004)27-42.
- [4] Maute K. and Reich G.W., Integrated multidisciplinary topology optimization approach to adaptive wing design, Journal of Aircraft, 43(1) (2006)253-263.
- [5] Afonso S.M.B., Sienz J. and Belblidia, F., Structural optimization strategies for simple and integrally stiffened plates and shells, Engineering Computations, 22(4) (2005)429-452.
- [6] Yin L. H., Fan S. Q. and Liu L. M. ,Optimization of the heat shield based on the sequential quadratic programming algorithm, CJK-OSM7. Huangshan, China, June 2012.
- [7] Kang Z., Wang X. M. and Wang R., Topology optimization of space vehicle structures considering attitude control effort, Finite Elements in Analysis and Design, 45 (2009)431-438.
- [8] Chen B.S., Kang G. J. and Li Y.P., Design optimization of stiffened storage tank for spacecraft, Structural and Multidisciplinary Optimization, 36(1) (2008)83--92.